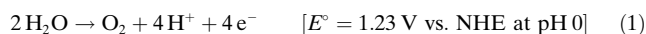


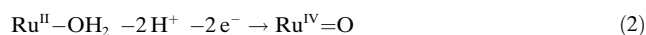
The *cis*-[Ru^{II}(bpy)₂(H₂O)₂]²⁺ Water-Oxidation Catalyst Revisited**

Xavier Sala, Mehmed Z. Ertem, Laura Vigarà, Tanya K. Todorova, Weizhong Chen, Reginaldo C. Rocha, Francesco Aquilante, Christopher J. Cramer,* Laura Gagliardi,* and Antoni Llobet*

The oxidation of water into molecular oxygen is of particular interest as one of the key reactions involved in solar energy conversion schemes based on the photoproduction of hydrogen from water and sunlight.^[1] There has been a dramatic surge of activity in this field recently and many new molecular Ru and Ir complexes have been described to catalyze the oxidation of water to dioxygen.^[2] One remaining challenge, however, is the elucidation of the mechanisms by which such water-oxidation reactions occur as well as the key factors that govern them.^[3] The mechanistic elucidation is a difficult task owing to the molecular complexity involved in this reaction that consists of the removal of four protons and four electrons from two water molecules and the formation of an oxygen–oxygen double bond [Eq. (1); NHE = normal hydrogen electrode].

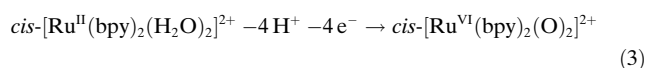


Most water-oxidation catalysts described to date cycle through some variation of the so-called Ru-aqua/Ru-oxo chemistry [as exemplified in Eq. (2)], taking advantage of the favorable energetics involved in proton-coupled electron-transfer processes.^[4]



Complexes containing two Ru–OH₂ bonds are thus of interest because they can potentially lose 4H⁺/4e[−], as in the case of *cis*-[Ru^{II}(bpy)₂(H₂O)₂]²⁺ (*cis*-**1**; bpy = 2,2′-bipyridine), thus leading to the formation of the Ru bis-oxo species *cis*-[Ru(bpy)₂(O)₂]²⁺ **2**, in which the Ru center may be assigned a formal oxidation state of +VI in the limit of viewing all oxidations taking place at the metal.^[5]

To better characterize the electronic structure of the formally bis-oxo Ru^{VI} state derived from *cis*-**1** [Eq. (3)] and its



implications for water-oxidation reactivity, M06-L DFT and CASSCF/CASPT2 calculations were undertaken (details in the Supporting Information). Analysis of the molecular orbitals (MOs) obtained from both levels of theory (shown in idealized form in Figure 1) suggests that the supported RuO₂ subsystem involves substantial covalency between the Ru and O atoms and includes a three-center-six-electron fragment, analogous to an organic allyl fragment (except that Ru contributes two atomic d orbitals to the hybrid MOs instead of one atomic p orbital). Thus, the formal Ru^{II} atom with six 4d electrons has two such electrons that by symmetry contribute only to Ru–O σ bonds, and four 4d electrons in the π system; the two O atoms each contribute one 2p electron to

[*] Dr. X. Sala, Dr. L. Vigarà, Prof. A. Llobet
Institute of Chemical Research of Catalonia (ICIQ)
Av. Països Catalans 16, 43007 Tarragona (Spain)
E-mail: allobet@iciq.es
M. Z. Ertem, Prof. C. J. Cramer, Prof. L. Gagliardi
Department of Chemistry and Supercomputing Institute
University of Minnesota
207 Pleasant St. SE, Minneapolis, MN 55455-0431 (USA)
E-mail: cramer@umn.edu
gagliardi@umn.edu
Dr. T. K. Todorova, Dr. F. Aquilante, Prof. L. Gagliardi
Département chimie physique, Université de Genève
30 Quai Ernest Ansermet, 1211 Geneva (Switzerland)
Dr. W. Chen, Dr. R. C. Rocha
Los Alamos National Laboratory, MPA-CINT
Los Alamos, NM 87545 (USA)
Prof. A. Llobet
Departament de Química, Universitat Autònoma de Barcelona
Cerdanyola del Vallès, 08193 Barcelona (Spain)

[**] Support was received from SOLAR-H2 (EU 212508) and the MICINN (Consolider Ingenio 2010 (CSD2006-0003, CTQ2007-67918)). C.J.C. and L.G. thank the U.S. NSF (CHE-0610183) and Swiss NSF (200021-111645/1). The work at Los Alamos was supported by the LANL-LDRD program. X.S. is grateful for a Torres Quevedo contract from MICINN. bpy = 2,2′-bipyridine.

Supporting information for this article is available on the WWW under <http://dx.doi.org/10.1002/anie.201002398>.

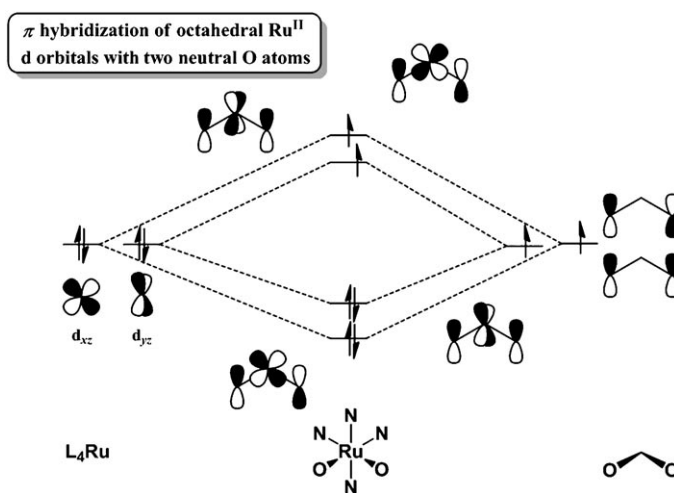


Figure 1. Hybridization of Ru d and O p orbitals resulting in net one-electron oxidation of Ru^{II}; triplet coupling is shown for simplicity.

the π system (the other five electrons on each O atom comprise two lone pairs and half of a Ru–O σ bond). The resulting hybridization of the π MOs leads to a narrow separation between the two highest energy orbitals shown in Figure 1, so that the singlet and triplet states are close to one another in energy (the singlet state is preferred by 3.9 and 4.6 kcal mol⁻¹ at the M06-L and CASSCF/CASPT2 levels, respectively).

The roughly even distribution of the six π electrons, over the four original atomic orbitals, leads to a net one-electron oxidation of the metal with that electron shared equally over both O atoms. That is, theory suggests that, considering only the π system, the optimal mesomeric representation of the *cis* bis-oxo species is $^-\text{O}-\text{Ru}^{\text{III}}-\text{O}^{\bullet} \leftrightarrow \bullet\text{O}-\text{Ru}^{\text{III}}-\text{O}^-$ or, equivalently, *cis*-[Ru^{III}(bpy)₂(O^{-0.5})₂]²⁺. While polarization of the covalent Ru–O σ bonds may contribute to some additional oxidation of Ru in **2**, the presence of unpaired spin density on the metal and the O atoms is consistent with electrophilic oxygen atoms.

Water oxidation with O₂ evolution following addition of excess Ce^{IV} to *cis*-**1** was originally thought to be a result of the formation of RuO₂ that appears as a black solid in the reaction vessel.^[5] However, from our systematic experiments with manometric monitoring of O₂, we clearly demonstrate here that *cis*-**1** is capable of catalytically producing dioxygen at a much faster rate than either RuO₂ or *trans*-**1** (Figure 2). The *trans*-**1** complex used in this work was independently prepared by photoisomerization of *cis*-**1**.^[5a]

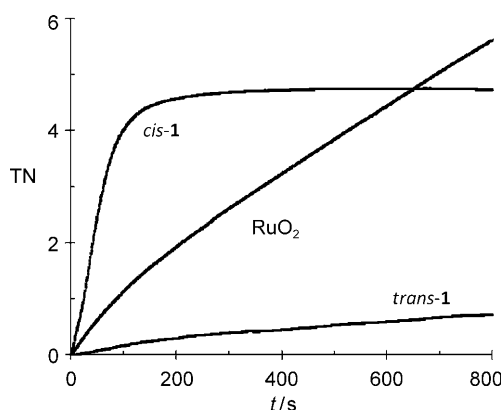


Figure 2. O₂-evolution profiles (TN = turnover number) for *cis*-**1**, *trans*-**1**, and RuO₂; [catalyst] = 1.0 mM and [Ce^{IV}] = 100 mM in 2.0 mL of a 0.1 M triflic acid solution (pH 1.0) at 298 K (for more details see the Supporting Information).

The much slower performance observed for *trans*-**1** reveals that the *cis* → *trans* isomerization process does not take place significantly in the absence of light under our working conditions. Ligand-loss chemistry producing RuO₂ has also been described for this system but it occurs at a much smaller rate (time scale of hours) compared to the rate observed for the water-oxidation reaction and, therefore, does not contribute here either. These alternative, potential reaction pathways for **2**, are depicted in Figure 3 and were all taken into consideration and carefully analyzed in this work.

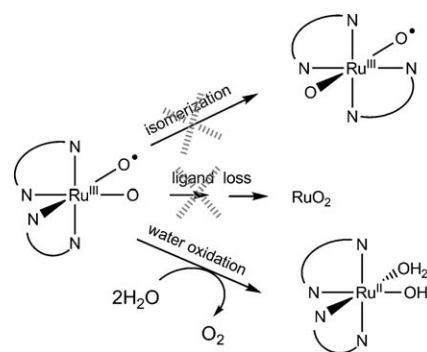


Figure 3. Reaction pathways for the oxidized, “bis-oxo” complex [Ru(bpy)₂(O)₂]²⁺. Formal oxidation states are indicated in the drawn structures of the complexes. Each N∩N represents a bpy ligand.

Although the performance of *cis*-**1** as a water-oxidation catalyst is limited to a handful of turnovers, the reactivity of this mononuclear complex toward O₂ evolution is very interesting from a mechanistic perspective because it gives very valuable information about the critical O–O bond-formation step following activation to its catalytically active “bis-oxo” state **2**.

To obtain such detailed mechanistic information, we carried out ¹⁸O-labeling experiments using different degrees of labeling for both the catalyst (*cis*-**1**) and the solvent (water). The experiments were designed so that only one turnover could take place; the produced gases were analyzed on-line by mass spectrometry (MS). The results of the labeling experiments are listed in Table 1, and their corresponding MS profiles are available in the Supporting Information. Our findings unambiguously demonstrated that the only mechanism operating in the case of *cis*-**1** is water nucleophilic attack (WNA), as depicted in the left catalytic cycle in Figure 4.

The experimentally determined preference for a WNA pathway was corroborated by both M06-L and CASSCF/CASPT2 calculations, from which the relative energetics of the possible mechanisms were also computed (Figure 4). Most notably, the activation free energies for WNA and intramolecular O–O bond closure are predicted to differ by 32.4 kcal mol⁻¹ in aqueous solution, with the latter being

Table 1: Relative isotopic ratios of O₂ evolved from the first metal cycle at different degrees of catalyst/solvent labeling, along with the calculated values assuming different reaction mechanisms.

Entry	¹⁸ O labeling [%] ^[a]		Isotopic ratios				
	Cat.	Solv.	O ₂	Exch ^[b]	Nuc ^[c]	Intra ^[d]	Exptl
1	–	19.4	¹⁶ O ₂	65.0	80.4	99.5	84.0
2	–	–	¹⁶ O ¹⁸ O	31.3	19.5	0.5	16.0
3	–	–	¹⁸ O ₂	3.8	0.05	6 × 10 ⁻⁴	1 × 10 ⁻²
4	19.4	9.7	¹⁶ O ₂	81.5	72.8	65.0	73.3
5	–	–	¹⁶ O ¹⁸ O	17.5	25.3	31.3	25.4
6	–	–	¹⁸ O ₂	0.9	1.9	3.8	1.3

[a] Degree of catalyst and solvent ¹⁸O labeling. [b] Exch: expected ratios in the case of a fast O atom exchange between the catalyst and the solvent. [c] Nuc: expected ratios for the mechanism involving a nucleophilic attack of a solvent water to the O atom of a Ru–O group. [d] Intra: expected ratios for the mechanism involving an intramolecular oxygen–oxygen coupling from the two Ru–O groups.

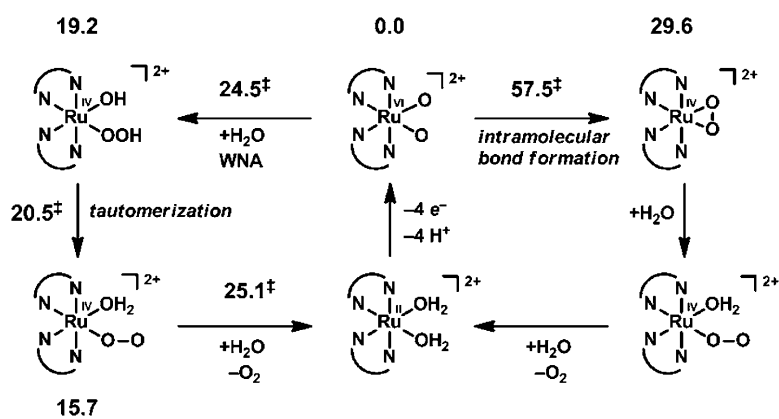


Figure 4. M06-L free energies (kcal mol⁻¹) including SMD aqueous solvation for WNA (left cycle) and intramolecular bond formation (right cycle); free energies of activation are indicated with a double-dagger. Formal oxidation states are indicated for easy electron counting purposes. SMD = solvation model density.

strongly disfavored because, with the unpaired spin density all in the π system, two O σ lone pairs of electrons must be driven together along the reaction coordinate (cf. Figure 1). The activation free energy for the WNA pathway is for a structure that includes a second water molecule that acts as a catalyst; its O atom behaves as a proton acceptor from the attacking water molecule and as a proton donor to the other O group on Ru. When the catalytic water is not included, the activation free energy is predicted to be 29.9 kcal mol⁻¹. The potential catalytic role of water molecules in such metal-catalyzed reactions was previously observed for the dinuclear water-oxidation catalyst *in, in*-[[Ru(tpy)(OH₂)₂(μ -bpp)]³⁺ (tpy = 2,2':6,2''-terpyridine and bpp = 3,5-bis(2-pyridyl)pyrazolate), for which the O–O bond-formation step in the catalytic cycle involves an intramolecular pathway.^[6] This instance manifests again the importance of hydrogen bonding in the stabilization of transition states for these types of reactions.^[7]

Gas-phase CASSCF/CASPT2 calculations also predict a strong preference for the first WNA step compared to intramolecular bond formation (about 40 kcal mol⁻¹). The remaining steps in the WNA pathway were also characterized and proceed with roughly similar activation free energies relative to the initial [Ru^{III}(bpy)₂(O^{-0.5})₂]²⁺ reactant (Figure 4), thus firmly establishing the viability of the WNA process. Based on kinetics analysis, a WNA mechanism has been previously invoked for the “blue dimer”, *cis, cis*-[[Ru^{III}(bpy)₂(OH₂)₂(μ -O)]⁴⁺,^[8] and for the mononuclear complexes [Ru^{II}(tpy)(L)(H₂O)]²⁺ (L = 2,2'-bypyrimidine or 2,2'-bypyrazine);^[9] labeling experiments for the “blue dimer” also indicated that its reaction occurs via multiple simultaneous pathways.^[8b–10]

In conclusion, we have established that *cis*-**1** acts as a water-oxidation catalyst when treated with excess Ce^{IV}.

Results of M06-L and CASSCF/CASPT2 calculations indicated that removal of 4H⁺ and 4e⁻ from *cis*-**1** leads to a reactive species in which the RuO₂ π system has unpaired spin density on both Ru and the O atoms, consistent with electrophilic O atoms and a Ru oxidation state below the formal limit of VI. ¹⁸O-labeling experiments combined with the theoretical characterization of the catalytic cycle provided definite evidence that the only operative catalytic mechanism involved is water nucleophilic attack on a Ru–O group. This work constitutes the first example where a direct experimental evidence for the nucleophilic attack single mechanism has been obtained in an unambiguous manner and thus represents a step forward in this field.

Received: April 22, 2010

Revised: July 14, 2010

Published online: September 6, 2010

Keywords: density functional calculations · energy conversion · reaction mechanisms · ruthenium · water oxidation

- [1] A. C. Benniston, A. Harriman, *Mater. Today* **2008**, *11*, 26–34.
- [2] a) J. Mola, E. Mas-Marza, X. Sala, I. Romero, M. Rodriguez, C. Vinas, T. Parella, A. Llobet, *Angew. Chem.* **2008**, *120*, 5914; *Angew. Chem. Int. Ed.* **2008**, *47*, 5830; b) Z. Chen, J. J. Concepcion, J. W. Jurss, T. J. Meyer, *J. Am. Chem. Soc.* **2009**, *131*, 15580; c) Y. V. Geletii, Z. Huang, Y. H. Djamaladdin, G. Musaev, T. Lian, C. L. Hill, *J. Am. Chem. Soc.* **2009**, *131*, 7522.
- [3] M. H. Huynh, T. J. Meyer, *Chem. Rev.* **2007**, *107*, 5004.
- [4] a) Z. Chen, J. J. Concepcion, X. Hu, W. Yang, P. G. Hoertz, T. J. Meyer, *Proc. Natl. Acad. Sci. USA* **2010**, *107*, 7225–7229; b) J. J. Concepcion, M.-K. Tsai, J. T. Muckerman, T. J. Meyer, *J. Am. Chem. Soc.* **2010**, *132*, 1545; c) S. Romain, L. Vigara, A. Llobet, *Acc. Chem. Res.* **2009**, *42*, 1944.
- [5] a) J. C. Dobson, T. J. Meyer, *Inorg. Chem.* **1988**, *27*, 3283; b) J. P. Collin, J. P. Sauvage, *Inorg. Chem.* **1986**, *25*, 135.
- [6] a) S. Romain, F. Bozoglian, X. Sala, A. Llobet, *J. Am. Chem. Soc.* **2009**, *131*, 2768; b) F. Bozoglian, S. Romain, M. Z. Ertem, T. K. Todorova, C. Sens, J. Mola, M. Rodríguez, I. Romero, J. Benet-Buchholz, X. Fontrodona, C. J. Cramer, L. Gagliardi, A. Llobet, *J. Am. Chem. Soc.* **2009**, *131*, 15176.
- [7] See also L. P. Wang, Q. Wu, T. Van Voorhis, *Inorg. Chem.* **2010**, *49*, 4543.
- [8] a) F. Liu, J. J. Concepcion, J. W. Jurss, T. Cardolaccia, J. L. Templeton, T. J. Meyer, *Inorg. Chem.* **2008**, *47*, 1727; b) H. Yamada, W. F. Siems, T. Koike, J. K. Hurst, *J. Am. Chem. Soc.* **2004**, *126*, 9786.
- [9] J. J. Concepcion, J. W. Jurss, J. L. Templeton, T. J. Meyer, *J. Am. Chem. Soc.* **2008**, *130*, 16462.
- [10] D. Geselowitz, T. J. Meyer, *Inorg. Chem.* **1990**, *29*, 3894.